Electronic theory of phase stability in substitutional alloys: The generalized perturbation method versus the Connolly-Williams method

M. Sluiter
Materials and Chemical Science Division, Lawrence Berkeley Laboratory, 1 Cyclotron Road, Berkeley, California 94720 and Condensed Matter Division (L-268), Lawrence Livermore National Laboratory, P.O. Box 808, Livermore, California 94550

P. E. A. Turchi
Condensed Matter Division (L-268), Lawrence Livermore National Laboratory, P.O. Box 808, Livermore, California 94550
(Received 26 May 1989)

A detailed analysis of the tendencies toward ordering and phase separation, and more generally the stability properties at $T \neq 0$ K in substitutional alloys, is carried out using the prescription proposed by Connolly and Williams and the generalized perturbation method. Both methods are examined and contrasted within the framework of a simple but realistic tight-binding model applicable to paramagnetic transition-metal alloys.

I. INTRODUCTION

The basic tools for studying ordering and phase stability in substitutional alloys and ultimately their phase diagrams, are based on the so-called 3D Ising model within various approximations, such as the cluster-variation method[1,2] (CVM) and Monte Carlo simulations.[3,4] In these models it is assumed that the internal energy can be written as a rapidly convergent sum of pair and multisite interactions. This statement has been proved in normal metals and their alloys[5] using the pseudopotential theory, but in transition metals, where strong disorder effects can be important, such an expansion must be clearly justified. Statistical mechanical studies of ordering processes, with arbitrarily chosen interactions, have been remarkably successful. The realization that these interactions can be derived from electronic band-structure calculations has initiated extensive research in an effort to provide a direct link with statistical-mechanical models. Among other approaches, one can mention the concentration functional theory of ordering,[6] the embedded-cluster method,[7] the generalized perturbation method[8] (GPM), the Connolly-Williams method[9] (CWM), and the closely related ε-G approach.[10,11] The aim of this paper is to examine and contrast two alloys theories, namely, the GPM and the CWM. This preliminary study is performed within a tight-binding framework applicable to paramagnetic transition metal alloys, but as will become apparent, the conclusions drawn from this study are expected to be model independent.

In the GPM a perturbation treatment is derived by choosing a reference medium which is close to any particular configuration of the alloy. Hence, the intuitive idea to use the completely disordered state, as the one described by the coherent-potential approximation (CPA),[12,13] as an appropriate reference medium.[8,14–19]

Let p_n^i be the occupation numbers, usually defined as $p_n^i = 0$ or 1 depending on whether or not site n is occupied by an atom of type i ($i = A,B$). Thus, for a binary alloy $A_{1-c}B_c$, in which only chemical rearrangements exist, each atomic configuration is completely specified by the set of $\{p_n^i\}$.

The GPM allows the band energy $E(\{p_n^i\})$ of a given configuration of the alloy to be expressed as the sum of two terms: (1) the energy of the totally disordered state, $E_{\rm dis}(c)$, also called the disordered energy, which is concentration dependent but independent of the set $\{p_n^i\}$ and hence configuration independent, and (2) the ordering energy $\Delta E_{\rm ord}(\{P_n^i\})$, which is the difference between the energy of the state specified by the set $\{p_n^i\}$ and the energy of the totally disordered state. It is important to note that the simplest version of GPM does not study the configuration dependence of the energy of alloying, or the total energy, but rather focuses only on one (important) contribution to the total energy, namely the band energy. The band energy is the main contribution to the total energy, in the absence of charge transfer, because other electronic contributions to the total energy either cancel (interatomic electron-electron energy and Madelung energy) or vanish (intra-atomic electron-electron energy). However, charge-transfer effects can be taken into account within the GPM description.[17,20] The band energy is given by

$$E(\{p_n^i\}) = E_{\rm dis}(c) + \Delta E_{\rm ord}(\{p_n^i\}) , \tag{1}$$

with

$$\Delta E_{\rm ord}(\{p_n^i\}) = \tfrac{1}{2} \sum_{n,m} V_{n,m}(c) \delta c_n \delta c_m + \tfrac{1}{3} \sum_{n,m,l} V_{n,m,l}(c) \delta c_n \delta c_m \delta c_l + \cdots , \tag{2}$$

where $c = c^B$ is the concentration of the B species, $\delta c_n = p_n^B - c^B$ is the concentration deviation at site n and $V_{n,\ldots}(c)$ is the concentration-dependent cluster interaction.

These cluster interactions, for a given lattice (fcc, bcc, ...), depend on the distances between the cluster

sites (n,m in case of pairs, n,m,l in case of triplets) and their relative arrangements, the concentration c, and the following electronic quantities: the one-electron potential difference $\varepsilon^A-\varepsilon^B$ and the Fermi energy ε_F which determines the filling of the band with respect to the completely disordered state, i.e., the averaged number of electrons per atom. Note that the concentration dependence of the cluster interactions reflects the properties of the reference medium and, therefore, the averaged local neighborhood of the clusters. Due to mean-free-path effects (scattering), a rapid convergence of the expansion is expected.

The CWM is based on a formal expression for the total energy, first derived by Sanchez (see, e.g., Ref. 21),

$$E^{\alpha}_{\rm tot}(r)=\sum_{\gamma}^{\infty} V_{\gamma}(r)\xi^{\alpha}_{\gamma} , \tag{3}$$

where the total energy of a particular configuration α is expressed as the sum of products of multisite interactions V_γ and multisite correlations ξ^α_γ. These correlations are defined as

$$\xi_{\gamma}=\frac{1}{N_{\gamma}}\sum_{\{n_i\}}\sigma_{n_1}\sigma_{n_2}\cdots\sigma_{n_{\gamma}} ,$$

where $\sigma_n=1-2p_n$, takes the values $+1$ or -1 depending on the occupancy of site n, N_γ is the total number of γ-type clusters, and the sum runs over all γ-type clusters on the lattice.

The total energies and the multisite interactions are generally lattice-parameter r (or volume) dependent. The multisite interactions are not composition dependent in an explicit fashion as in the GPM. However, the CWM interactions vary indirectly with composition because the equilibrium volume is generally composition dependent. The summation in (3) runs over all clusters types that can be formed by combining sites on the entire crystal (including the "empty" cluster).

Provided that the configurations are restricted to ordered structures, total energies can be computed by accurate *ab initio* band-structure methods, and multisite correlations (which are determined by site occupancy only) can be found by inspection. The computation of V_γ proceeds by inversion of the system (3). In practice, (3) can be solved only if the existence of a maximum cluster $\gamma_{\rm max}$ is assumed beyond which the corresponding multisite interactions are supposed to be negligible. Hence, by choosing a set of ordered structures and by (arbitrarily) truncating the summation in (3) a set of multisite interactions can be obtained from,

$$\begin{aligned} &V_{\gamma}(r)=\sum_{\alpha}(\xi^{\alpha}_{\gamma})^{-1}E^{\alpha}_{\rm tot}(r), \quad \phi\le\gamma\le\gamma_{\rm max} ,\\ &V_{\gamma}(r)=0, \quad \gamma_{\rm max}<\gamma<\infty , \end{aligned} \tag{4}$$

where ϕ represents the empty cluster.

The empty- and point-cluster "interactions" do not affect coherent phase diagrams, or more general, phase equilibria. When comparing superstructures based on different lattices, the respective differences between the empty- and point-cluster interactions must be taken into account. These two interactions merely supply an energy contribution that is linear in composition. Hence, it follows that instead of using total energies to compute the cluster interactions (beyond the point cluster), any other energy can be used to compute the interactions as long as it satisfies the condition that it only differs from the total energy merely by a linear function of composition. The band energy satisfies that condition assuming that charge-transfer and zero-point vibrational effects can be neglected. Therefore, the band energy will be used instead of the total energy from now on. For simplicity the band energies will be calculated at fixed volume.

The disordered energy, playing a crucial role in the GPM, is obtained as a by-product in the CWM. In the totally disordered state the pair- and higher-order correlations are given as products of the point correlations. In a disordered structure with one atom per unit cell, such as fcc and bcc, all atomic positions are equivalent so that all correlations can be expressed in terms of one point correlation ξ_1:

$$\xi^{\rm dis}_{\gamma}=(\xi_1)^{n_\gamma} ,$$

where n_γ is the number of sites contained in the γ cluster. The energy of the disordered configuration, according to the CWM, is then given by

$$E^{\rm dis}_{\rm tot}=\sum_{\gamma}^{\gamma_{\rm max}} V_{\gamma}(\xi_1)^{n_\gamma} . \tag{5}$$

We have extended the CWM in various ways. (1) Other ordered structures than the ones originally proposed (fcc, $L1_0$, $L1_2$) have been included. The set has been extended with the following set of ordered structures: DO_{22} (A_3B and AB_3), $MoPt_2$ type of order (A_2B and AB_2), A_2B_2 (phase 40 in Kanamori's notation[22]), $L1_1$ (CuPt prototype) (AB), and Pt_8V type of order (A_8B) (see Ref. 22 for a description of these ordered structures). This allows computation of cluster interactions from various sets of ordered structures (called basis sets from now on), i.e., including other combinations than the usual set A, B, $L1_2$ and $L1_0$. (2) Expansion (3) has been truncated at the tetrahedron-octahedron (TO) maximum cluster, which leads to a set of 11 interactions V_γ as opposed to a set of only 5 interactions at the tetrahedron (T) maximum-cluster truncation. (3) Moreover, the case of overdetermined systems is considered where interactions are obtained from a large set of ordered structures by a least-squares fit. In general, one expects that this will lead to an improved accuracy of the cluster interactions since the effects of the arbitrary truncation at the maximum cluster in (3) are "averaged out."

An alternate method of determining cluster interactions is to find two ordered structures that have identical correlations, except for the cluster which interaction is to be determined. Because of geometrical constraints, this is strictly speaking not possible. However, one can find structures which have identical correlations (with exception for one cluster) up to quite a large maximum cluster. An example is formed by the $L1_1$ structure (CuPt prototype) and a structure defined as follows: A sites: $\frac{1}{2}0\frac{1}{2}$, $\frac{1}{2}\frac{1}{2}0$, 000, $0-\frac{1}{2}\frac{1}{2}$, B sites: $0\frac{1}{2}\frac{1}{2}$, $-\frac{1}{2}0\frac{1}{2}$, $-\frac{1}{2}\frac{1}{2}0$, 001, with

TABLE I. Correlations included in the tetrahedron truncation of the CWM for some structures on the bcc lattice. The ξ_i with increasing index i, correspond to the "empty" cluster, the point, the nearest-neighbor (NN) pair, the next-nearest-neighbor (NNN) pair, the triangle formed by two NN pairs and one NNN pair, and the tetrahedron formed by four NN pairs and two NNN pairs.

Structure	Composition	ξ_0	ξ_1	ξ_2	ξ_3	ξ_4	ξ_5
bcc	A	1	1	1	1	1	1
bcc	B	1	−1	1	1	−1	1
$B2$	AB	1	0	−1	1	0	1
$B32$	AB	1	0	0	−1	0	1
DO_3	A_3B	1	$\frac{1}{2}$	0	0	$-\frac{1}{2}$	−1
DO_3	A_3B	1	$-\frac{1}{2}$	0	0	$\frac{1}{2}$	−1

translation vectors ⟨110⟩, ⟨101⟩, and ⟨011⟩. These two structures have identical correlations up to the TO truncation except for the tetrahedron; there, the first structure has a correlation of −1 and the latter has a correlation of +1. Hence, to a good approximation, the difference of the two total energies should yield a good estimate for twice the tetrahedron cluster interaction. This alternate method is planned to be discussed in forthcoming work.

Correlations for the most common bcc and fcc based superstructures are given below in Tables I and II, respectively. Correlations for the empty cluster ξ_0 (not indicated in Table II) take the value unity for all structures. Correlations corresponding to the tetrahedron approximation of the CWM for fcc based structures can be extracted from Table II, by taking solely the coefficients corresponding to ξ_1, ξ_2, ξ_4, and ξ_6. A comparison of the correlations up to the tetrahedron maximum cluster indicates that the $L1_2$ and DO_{22} structures, and the $L1_0$ and "40" structures are degenerate.

To shorten the notation, the ordered structures, comprising the "basis sets," will be referred to by a number. The numbers are assigned as follows: $1=A$ −fcc, $2=B$ −fcc, $3=L1_0$, 4=40, $5=L1_1$, $6=A_2B$ −$MoPt_2$, $7=AB_2$ −$MoPt_2$, $8=A_3B-L1_2$, $9=AB_3-L1_2$, $10=A_3B-DO_{22}$, $11=AB_3-DO_{22}$, $12=A_8B-Pt_8V$, and $13=AB_8-Pt_8V$. Cluster interactions obtained with TO truncation with a basis set 1 through 13 thus correspond to a set of 11 cluster interactions obtained by a least-squares fit to the total energies of all structures corresponding to numbers 1 to 13. For brevity, this procedure will be denoted by TO:1–13. The commonly

TABLE II. Correlations included in the tetrahedron-octahedron truncation of the CWM for some structures on the fcc lattice. The ξ_i with increasing index i, correspond to the point, the nearest-neighbor (NN) pair, the next-nearest-neighbor (NNN) pair, the equilateral NN triangle, the isosceles triangle formed by one NNN and two NN pairs, the equilateral NN tetrahedron, the irregular tetrahedron consisting of one NNN and five NN pairs, the square formed by four NN pairs, the pyramid, and the octahedron, respectively. The abbreviations "comp." and "str." denote composition and structure.

comp.-str.	ξ_1	ξ_2	ξ_3	ξ_4	ξ_5	ξ_6	ξ_7	ξ_8	ξ_9	ξ_{10}
A-fcc	1	1	1	1	1	1	1	1	1	1
B-fcc	−1	1	1	−1	−1	1	1	1	−1	1
AB-$L1_0$	0	$-\frac{1}{3}$	1	0	0	1	$-\frac{1}{3}$	1	0	1
AB-40	0	$-\frac{1}{3}$	$\frac{1}{3}$	0	0	1	$\frac{1}{3}$	$-\frac{1}{3}$	0	−1
AB-$L1_1$	0	0	−1	0	0	−1	0	1	0	−1
A_2B-$MoPt_2$	$\frac{1}{3}$	$-\frac{1}{9}$	$\frac{1}{9}$	$-\frac{1}{3}$	$-\frac{1}{9}$	$-\frac{1}{3}$	$-\frac{1}{9}$	$\frac{1}{9}$	$\frac{1}{3}$	1
AB_2-$MoPt_2$	$-\frac{1}{3}$	$-\frac{1}{9}$	$\frac{1}{9}$	$\frac{1}{3}$	$\frac{1}{9}$	$-\frac{1}{3}$	$-\frac{1}{9}$	$\frac{1}{9}$	$-\frac{1}{3}$	1
A_3B-$L1_2$	$\frac{1}{2}$	0	1	$-\frac{1}{2}$	$\frac{1}{2}$	−1	0	1	$\frac{1}{2}$	1
AB_3-$L1_2$	$-\frac{1}{2}$	0	1	$\frac{1}{2}$	$-\frac{1}{2}$	−1	0	1	$-\frac{1}{2}$	1
A_3B-DO_{22}	$\frac{1}{2}$	0	$\frac{2}{3}$	$-\frac{1}{2}$	$\frac{1}{6}$	−1	$-\frac{1}{3}$	$\frac{1}{3}$	$-\frac{1}{6}$	0
AB_3-DO_{22}	$-\frac{1}{2}$	0	$\frac{2}{3}$	$\frac{1}{2}$	$-\frac{1}{6}$	−1	$-\frac{1}{3}$	$\frac{1}{3}$	$\frac{1}{6}$	0
A_5B ($C2/m$)	$\frac{2}{3}$	$\frac{1}{3}$	$\frac{1}{3}$	0	0	$-\frac{1}{3}$	$-\frac{1}{3}$	$-\frac{1}{3}$	$-\frac{2}{3}$	−1
AB_5 ($C2/m$)	$-\frac{2}{3}$	$\frac{1}{3}$	$\frac{1}{3}$	0	0	$-\frac{1}{3}$	$-\frac{1}{3}$	$-\frac{1}{3}$	$\frac{2}{3}$	−1
A_2B ($C2/m$)	$\frac{1}{3}$	0	$-\frac{1}{3}$	0	$-\frac{1}{3}$	$\frac{1}{3}$	0	$-\frac{1}{3}$	$\frac{1}{3}$	1
AB_2 ($C2/m$)	$-\frac{1}{3}$	0	$-\frac{1}{3}$	0	$\frac{1}{3}$	$\frac{1}{3}$	0	$-\frac{1}{3}$	$-\frac{1}{3}$	1
A_8B-Pt_8V	$\frac{7}{9}$	$\frac{5}{9}$	$\frac{19}{27}$	$\frac{1}{3}$	$\frac{13}{27}$	$\frac{1}{9}$	$\frac{7}{27}$	$\frac{11}{27}$	$\frac{5}{27}$	$\frac{1}{9}$
AB_8-Pt_8V	$-\frac{7}{9}$	$\frac{5}{9}$	$\frac{19}{27}$	$-\frac{1}{3}$	$-\frac{13}{27}$	$\frac{1}{9}$	$\frac{7}{27}$	$\frac{11}{27}$	$-\frac{5}{27}$	$\frac{1}{9}$

selected basis set[9,10,23–25] consisting of the pure metals, $L1_0$ and $L1_2$ ordered structures with T truncation corresponds to T:1,2,3,8,9.

Note that the CWM approach and the GPM are, in many respects, almost complete opposites as will be discussed in more detail below. The strength of the CWM lies in its flexibility: Any method can be used to obtain the total energies required as input, and in its simplicity the interactions are computed through solving a small system of linear equations. Furthermore, the effects of important physical variables such as lattice parameters can be included easily in the formulation of the multisite interactions. As an example, the influence of volume is demonstrated in the Appendix.

The GPM is based on a sound perturbative treatment of the disordered medium and produces uniquely defined concentration-dependent interactions. In the GPM, pair interactions tend to be significantly larger than multisite interactions, and among the pair interactions the first-neighbor interaction is usually much larger than the other pair interactions.[26–28]

The CWM on the other hand, does not uniquely define interactions. Rather, concentration-independent interactions are determined such that total energies of an arbitrarily chosen set of ordered configurations are reproduced by a rather arbitrarily truncated sum (3). It is clear that there is no guarantee whatsoever that choosing a different set of ordered structures or choosing another maximum cluster for truncation will reproduce previously computed interactions. However, if the concentration-independent multisite interactions do decay rapidly, as is assumed in the CWM, one can expect that previously mentioned ambiguities are minor and that in practice the interactions can be uniquely computed. These considerations bring up the following questions: (1) Is truncation of (3) justified, i.e., are the multsite interactions rapidly diminishing, and closely related, (2) to what extent do the CWM interactions vary if they are computed with total energies from different sets of ordered structures? (3) How do the CWM cluster interactions compare to GPM pair interactions? (4) How accurate are predictions of formation energies (or total energies) with the GPM and with the CWM, respectively? (5) Do phase diagrams computed with different sets of interactions from the CWM and the GPM resemble each other? Although the CWM has received much attention recently,[10,11,23–25,29–31] these crucial questions have been addressed only partly.[32]

In order to compare the CWM and the GPM on the same footing, a simple tight-binding model was used to study phase stability from band-structure calculations in binary substitutional paramagnetic transition-metal alloys. This tight-binding model has been studied in more detail elsewhere.[19,26–28,33]

II. FORMALISM

As usual, it will be assumed that the most important properties of a given transition-metal alloy $A_{1-c}B_c$ come from the d band. Hence, only d electrons will be taken into account. Within the complete orthogonal d-atomic orbital basis, the following tight-binding Hamiltonian will be used to describe the alloy in a particular configuration $\{p_n^i\}$:

$$H=\sum_{n,\lambda}|n\lambda\rangle\varepsilon_n^{\lambda}\langle n\lambda|+\sum_{n,m,\lambda,\mu}|n\lambda\rangle\beta_{nm}^{\lambda\mu}\langle m\mu|\ ,$$

where ε_n^{λ} is the orbital-dependent energy of the atomic level at site n, and $\beta_{nm}^{\lambda\mu}$ is the hopping integral between sites n and m, with orbital $\lambda(\mu)$ centered on site $n(m)$. Neglecting the d-orbital dependence of the energies ε_n^{λ} is a reasonable approximation in the case of transition metals. Thus, a site-occupancy dependent on-site energy ε_n, which takes the value ε^A (ε^B) if site n is occupied by an A (B) atom, specifies a given configuration of the alloy. For simplicity, the hopping integrals are assumed to be independent of site occupancy, and charge transfer effects are neglected. The alloy effects come in through the difference in the atomic d levels, also called the diagonal-disorder parameter: $\delta_d=(\varepsilon_B-\varepsilon_A)/\overline{W}$, where $\overline{W}$ is the concentration weighted average of the half d-band widths of the pure elements. In the following δ_d takes the value 0.8.

Canonical Slater-Koster parameters involving first nearest-neighbor hopping integrals in the fcc crystal structure will be used, $dd\sigma=-1.385$, $dd\pi=|dd\sigma|/2$, $dd\delta=0$, leading to a d-band width of 11.08 canonical units (c.u.) for the pure metal. Because of the spin degeneracy and the number of d orbitals a factor of 10 must be taken into account for all energetic properties. Therefore, for a typical d-band width of about 5 eV, 1 c.u. corresponds to approximately 10 $(5/11.08)\approx 4.5$ eV/atom (or conversely, 1 c.u. ≈ 0.45 eV/state).

The Green functions of the pure elements and the ordered superstructures, required for the CPA and GPM, and the CWM band energies, respectively, are computed with the recursion method.[34] The continued fraction expansion of the Green function is calculated with 11 exact levels and is terminated analytically according to the Beer-Pettifor method.[35] The band energy E_{band} (per atom) can be expressed as

$$E_{\text{band}}=\int_{-\infty}^{\varepsilon_F}d\varepsilon(\varepsilon-\varepsilon_F)n(\varepsilon)\ ,$$

where ε is the energy, and ε_F and $n(\varepsilon)$ are the Fermi level and the density of states (DOS), respectively, pertaining to the disordered alloy.

A similar expression is used for the band energies of ordered structures, which are required as input for the CWM. The DOS obtained for the various phases considered in this study are shown in Fig. 1. Within the context of this model, band energies for ordered structures computed with the recursion method can be regarded as exact.

For the tight-binding model previously outlined, analytic expressions for the GPM effective cluster interactions, mentioned in Eq. (2), can be derived. Note, that the GPM is by no means limited to the tight-binding approximation, see Ref. 36 for an application of the GPM within the multiple scattering formalism of the Korringa-Kohn-Rostoker–CPA (KKR-CPA) method. The configuration-dependent Hamiltonian can be written

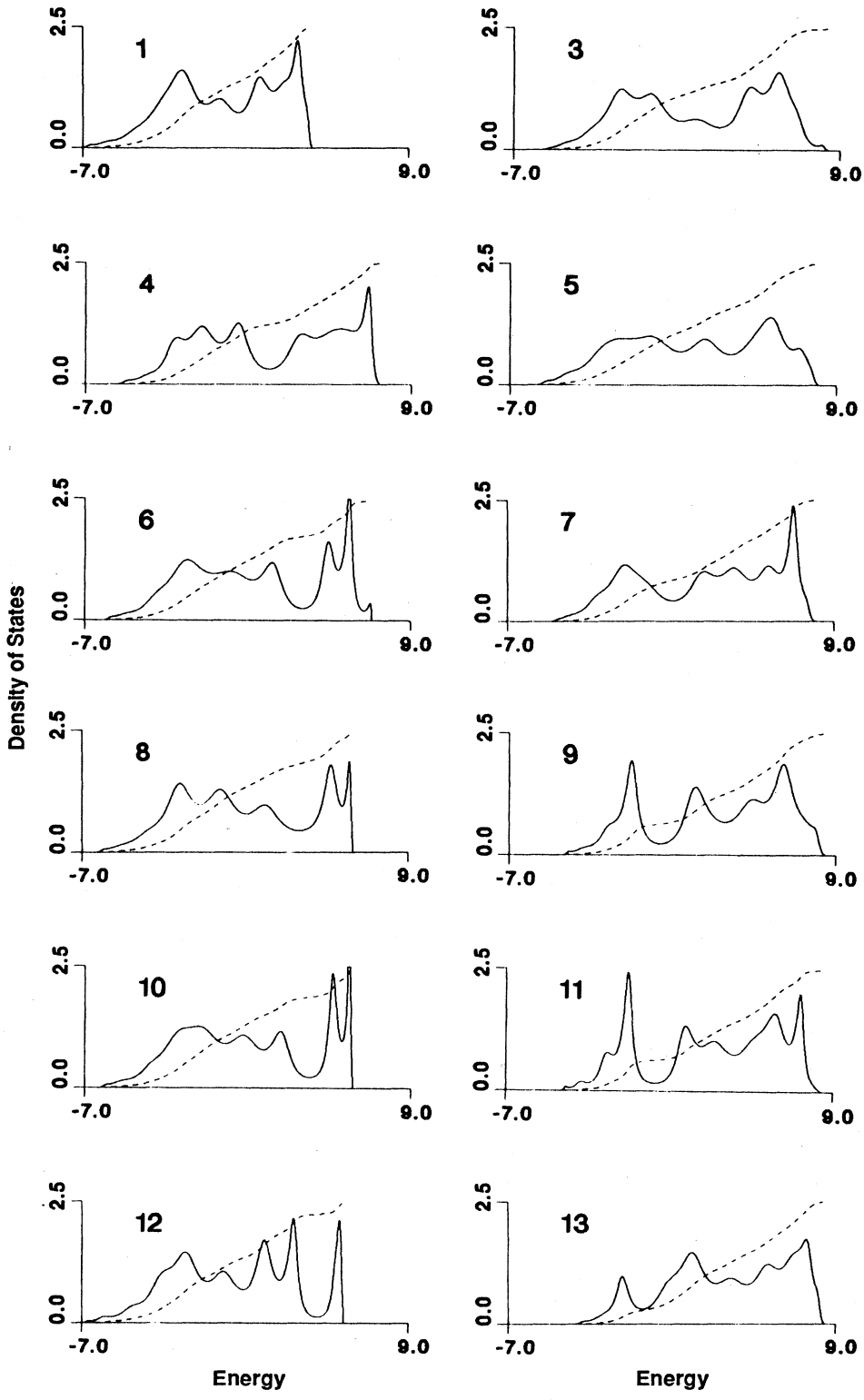

FIG. 1. Density of states for various fcc superstructures computed with the recursion method (11 levels of continued fraction, see the text). The solid line represents the density of states in states per canonical unit, and the dashed line indicates the band filling divided by 4 (the density of states are normalized to ten states). The numbers are assigned as follows: $1=A$ —fcc, $3=L1_0$, $4=40$, $5=L1_1$, $6=A_2B$ —$MoPt_2$, $7=AB_2$ —$MoPt_2$, $8=A_3B-L1_2$, $9=AB_3-L1_2$, $10=A_3B-DO_{22}$, $11=AB_3-DO_{22}$, $12=A_8B-Pt_8V$, and $13=AB_8-Pt_8V$. Number 2, corresponding to B —fcc, is the same as number 1 except for a shift of the energy axis by 4.16 canonical units.

as a perturbation of the CPA medium,

$$H = h + h^* ,$$

with

$$h = \sum_{n,\lambda} |n\lambda\rangle \Sigma \langle n\lambda| + \sum_{n,m,\lambda,\mu} |n\lambda\rangle \beta_{nm}^{\lambda\mu} \langle m\mu|$$

and

$$h^* = \sum_{n,\lambda} |n\lambda\rangle (\varepsilon_n - \Sigma) \langle n\lambda| ,$$

where h is the Hamiltonian of the CPA medium, h^* is the configuration-dependent perturbation term, and Σ is, for simplicity, the orbital-independent CPA self-energy. The CPA self-energy is site independent for the lattice under consideration (fcc). Note that the alloy Hamiltonian H, which has no translational symmetry, is split in two parts: the translationally invariant CPA Hamiltonian h, and the site-diagonal perturbative term h^*, which carries all configuration dependence. This separation allows the band energy to be written as a configuration-dependent perturbation expansion.[27] The expansion coefficients in the expression for the ordering energy (2), that is, the effective cluster interactions V, are given by

$$V_n^i = \frac{1}{5\pi} \mathrm{Im} \int^{\varepsilon_F} d\varepsilon \sum_{\lambda} \ln[1 - (\varepsilon^i - \Sigma) F^{\lambda}] ,$$

$$V_{nm}^{ij} = -\frac{1}{5\pi} \mathrm{Im} \int^{\varepsilon_F} d\varepsilon \, t^i t^j \sum_{\lambda,\mu} g_{nm}^{\lambda\mu} g_{nm}^{\mu\lambda} ,$$

where i,j represent either element A or B, F is the site-diagonal Green function, t is a (site) diagonal element of the scattering matrix, and g is the (site) off-diagonal Green function. The single-site interactions allow species to preferentially occupy certain sites. When all sites in the unperturbed medium are equivalent, as in this study pertaining to the fcc lattice, the single-site interaction term of the ordering energy expansion vanishes according to

$$\sum_{i,n} (p_n^i - c^i) V^i = \sum_i V^i \sum_n (p_n^i - c^i) = 0 .$$

The expression for the ordering energy can be simplified even more (i) by using the relations $\sum_i p_n^i = 1$, hence $p_n^A = 1 - p_n$, where p_n and c from now on will refer to the B species only, and (ii) by defining $\Delta t = t^B - t^A$. This algebraic manipulation yields

$$\Delta E_{\mathrm{ord}}(\{p_n\}) = \frac{1}{2N} \sum_{nm} (p_n - c)(p_m - c) V_{nm} + \cdots ,$$

where the effective-pair interactions (EPI) V_{nm} are given by

$$V_{nm} = V_{nm}^{AA} - V_{nm}^{AB} - V_{nm}^{BA} + V_{nm}^{BB}$$
$$= -\frac{1}{5\pi} \mathrm{Im} \int^{\varepsilon_F} d\varepsilon (\Delta t)^2 \sum_{\lambda,\mu} (g_{mn}^{\lambda,\mu})^2 .$$

Retaining only the effective-pair interaction terms results in a simple equation for the ordering energy

$$\Delta E_{\mathrm{ord}}(\{q_s\}) = \sum_s q_s V_s , \tag{6}$$

where V_s is the effective-pair interaction between an atom and its neighbor in the sth coordination shell, and q_s is a coefficient which depends on the occupation of the sth neighbor shell of a B atom in the alloy, i.e., on the type of ordering. q_s is defined by

$$q_s = \tfrac{1}{2}(n_s^{BB} c - n_s c^2) , \tag{7}$$

where n_s is the number of sites in the s shell, n_s^{BB} is the number of B atoms in the s shell that surround a B atom at the origin.

The EPI (V_s) for a given lattice depend on (i) the composition (via the concentration-dependent self-energy of the CPA medium), (ii) the interatomic distance, (iii) the diagonal disorder δ_d, (iv) possibly on the off-diagonal disorder, in cases where the bandwidths of the two components of the alloy differ substantially, and (v) on the average filling of the d band N_e. Thus, we have

$$V_s = \overline{W} V(s, c, \delta_d, \delta_{nd}, N_e) ,$$

where

$$N_e = \int^{\varepsilon_F} d\varepsilon \, n_{\mathrm{dis}}(\varepsilon) ,$$

n_{dis} being the DOS of the disordered alloy (CPA medium). Note,

$$N_e = (1 - c) N_A + c N_B$$

where $N_{A\,(B)}$ is the number of d electrons per A (B) atom. The off-diagonal effect can be taken into account by allowing the hopping integrals to be site-occupation dependent[37] and by using a CPA adapted to this effect.[33]

In the tight-binding description, briefly outlined above, most of the tendencies toward ordering and phase separation as well as the prediction of the most probable ordered states at $T = 0$ K can be obtained with the GPM.[19,28] As in the extensive study performed by Bieber and Gautier,[28] the GPM expression for the ordering energy (2) is computed with two levels of truncation; only the point and pair contributions are considered [first two terms in Eq. (2)], and the pair interactions are computed up to the fourth nearest-neighbor shell [truncation of the summation in second term of Eq. (2)].

III. RESULTS AND DISCUSSION

A. Convergence of the CWM and GPM interactions

As mentioned earlier, the CWM requires a rapid convergence of expansion (3) in order to justify its truncation. This convergence is examined by computing CWM multisite interactions with both T and TO truncation and various basis sets of ordered structures.

First, the commonly chosen basis set[9,10,23–25] of pure metals A and B, $L1_0$ and $L1_2$ ordered structures with tetrahedron truncation (T:1,2,3,8,9) will be investigated. In Fig. 2 the pair, triangle, and tetrahedron cluster interactions (V_2, V_4, and V_6, respectively) are shown as a function of the number of d electrons of the B species for fixed $\Delta N = N_A - N_B$. Because of the proportionality between δ_d and ΔN, a value of $\Delta N = 6$ is chosen, in reason-

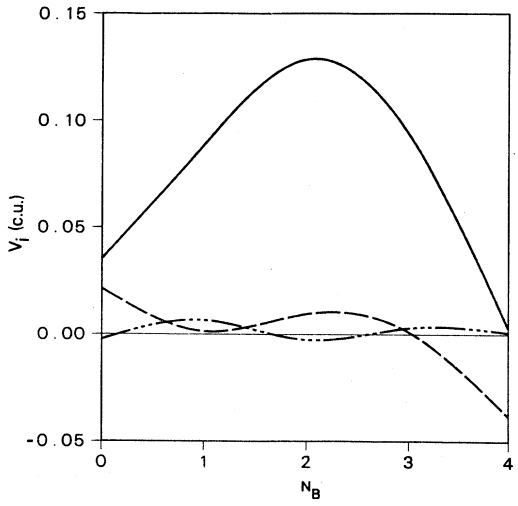

FIG. 2. CWM cluster interactions in canonical units computed with tetrahedron truncation and energies of the fcc, $L1_2$, and $L1_0$ phases; solid line: V_2, dashed line: V_4, and dash–triple-dotted line: V_6. The interactions are depicted as a function of the number of d electrons of element B ($N_B = N_A - 6$).

able agreement with $\delta_d = 0.8$. Convergence appears to be satisfactory since V_4 and V_6 are much smaller than V_2, except for very small and very large values of N_B. In the cases where the convergence is poor, the ordering of phases 3, 8, and 9 can be shown to be very small.

Figures 3(a) and 3(b) show the V_γ, $\gamma = 2,3,\ldots,10$ computed with TO:1–11. A similar pattern as was observed in Fig. 2 emerges, the first-neighbor-pair interaction (V_2) is much larger than all other interactions except when N_B is very small or very large, or, in other words, when the ordering energy is small. The interactions corresponding to the pyramid and octahedron (V_9 and V_{10}) are found to be significantly smaller than the other interactions.

Table III allows a more quantitative evaluation of the convergence. Cluster interactions obtained with T and TO truncation and various basis sets are listed for a {9-3} alloy, where, by convention, {9-3} stands for $N_A = 9$ and

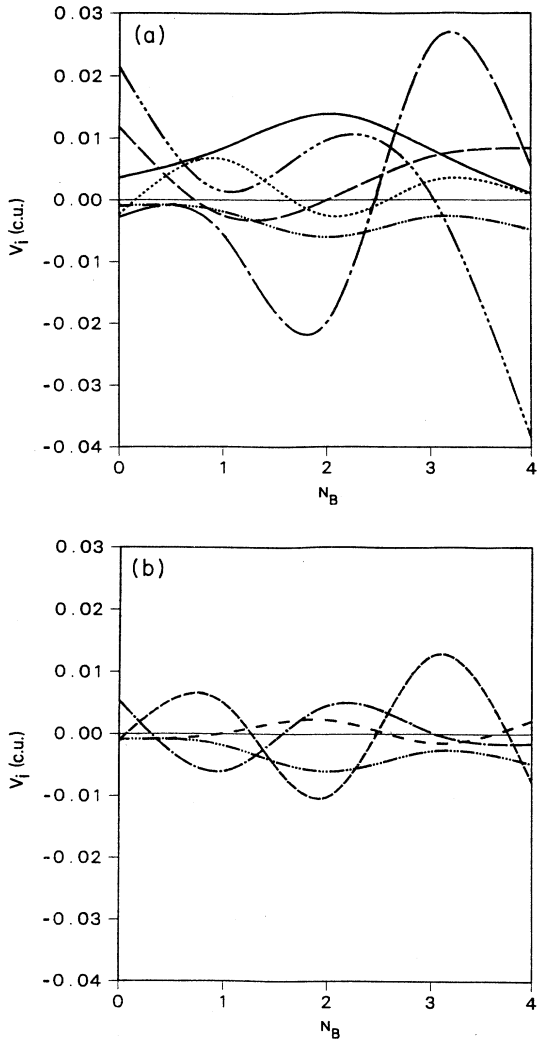

FIG. 3. CWM cluster interactions in canonical units, computed with tetrahedron-octahedron truncation: (a) ——$= 0.1 \times V_2$; – – – $= V_3$; ——·——$= V_4$; –·–·–·–$= V_5$; · · · ·$= V_6$; (b) ----$= V_7$; –···–···$= V_8$; ——-——$= V_9$; – – – $= V_{10}$. The interactions are shown as a function of $N_B (N_B = N_A - 6)$.

TABLE III. Cluster interactions V_γ (in canonical units), computed with T and TO truncation, for an alloy with $N_A = 9$ and $N_B = 3$, obtained with various basis sets: (a) T:1,2,3,8,9, (b) T:1,2,3,9,10, (c) T:1,2,4,10,11, (d) T:1–13, (e) TO:1–11, and (f) TO:1–13.

k	a	b	c	d	e	f
0	−0.136 650	−0.139 530	−0.134 370	−0.136 496	−0.139 330	−0.137 650
1	−0.332 896	−0.338 656	−0.341 270	−0.336 618	−0.357 759	−0.345 760
2	0.094 554	0.094 554	0.086 849	0.093 150	0.082 130	0.089 258
3					0.006 897	0.007 388
4	0.001 183	0.006 943	0.009 557	0.008 152	0.001 183	0.005 182
5					0.024 603	0.020 911
6	0.002 987	0.005 867	0.008 413	0.006 573	0.002 987	0.003 847
7					0.012 425	0.006 525
8					−0.002 767	−0.004 242
9					0.000 260	−0.008 969
10					−0.001 449	−0.002 597

$N_B=3$. The ratio of V_2 over V_6 takes values between 10.3 and 31.7, indicating that the first-neighbor-pair interaction is an order of magnitude greater than the tetrahedron interaction. The {9-3} alloy is not a special favorable case, the {8-2} alloy would yield even larger ratios. The {10-4} and the (hypothetical) {6-0} (Ref. 38) alloys, however, which have very small ordering energies, produce ratios of the order of unity, indicating a very poor convergence.

Note, that the absolute value of the ratio of V_6 over V_{10} is only about 1.5 to 2. This means that the convergence for larger clusters slows down considerably. In summary, it appears that the cluster interactions converge quite well, except when the ordering energies are small, in which case the first-neighbor interaction is not significantly larger than the other multisite interactions. Some general rules of thumb for the occurrence of small ordering energies in transition-metal alloys are given in Ref. 39.

A close inspection of Figs. 2, 3(a), and 3(b) and of Table III reveals that an important interaction is left out in the T truncation: the interaction V_5, associated with the irregular triangle, is quite large, larger than both the regular triangle and the tetrahedron interactions. The occurrence of such a large interaction cannot be known until the cluster interactions are computed with a larger maximum-cluster truncation, but at this higher level, once again, important interactions may have been excluded. Hence, it appears that one can never be certain that all significant interactions have been included in the computation of the cluster interactions.

For comparison, the convergence of the GPM effective-pair interactions is illustrated for a number of alloys in Table IV. The GPM yields pair interactions which converge extremely well when nearest-neighbor interactions are compared with more distant pairs. Averaged for the {7-1}, {8-2}, and {9-3} alloys, the absolute values of the ratios of V_1^{GPM} over V_2^{GPM}, V_3^{GPM}, and V_4^{GPM} are, respectively, 17.9, 34.1, and 18.1. This convergence is lacking for the {6-0} and, to a lesser extent, for the {10-4} alloys, where the V_1^{GPM} approaches zero. These two alloys were found to be problematic in the CWM also. In both methods the poor convergence of the interactions can be attributed to the smallness of the ordering energies. Aside from these "troublesome" alloys, the convergence beyond the nearest neighbor is extremely slow, V_2^{GPM}, V_3^{GPM}, and V_4^{GPM} are all of the same order of magnitude.

Concerning the convergence of the GPM interactions the following can be concluded: (1) The nearest-neighbor pair interaction is generally much larger than the interactions pertaining to more distant pairs. The more distant pair interactions do not converge rapidly, as V_2, V_3, and V_4 are all of the same order of magnitude. It must be noted, however, that the more distant pair interactions are extremely small, typically about 0.003 c.u. (0.014 eV), whereas the nearest-neighbor pair interaction is typically about 0.04 c.u. (0.18 eV). (2) The GPM interactions do not converge well when the nearest-neighbor interaction is very small, that is, when the ordering energy is small.

B. Uniqueness of the CWM cluster interactions

Table III allows a comparison of cluster interactions computed from various basis sets and with two levels of truncation: T and TO. With T-truncation, the largest and smallest values of the nearest-neighbor-pair interaction V_2 differ by less than 9%. The triangle and tetrahedron interactions V_4 and V_6, vary much more strongly; the ratio of the largest and the smallest values is as large as 8.1 and 2.8, respectively. The interactions, obtained with T or TO truncation, do not differ more from each other than the interactions obtained with T truncation vary among themselves. The multisite cluster interactions, computed with TO truncation, vary significantly percentage wise. In the case of V_9 the sign is different for basis sets 1–11 and 1–13. The absolute variation in the interactions V_γ does not appear to change with γ. Typically this variation takes values of about 0.004 canonical units (c.u.) with TO truncation, and about 0.007 c.u. with T truncation. It is clear then, that the CWM cluster interactions of small amplitude will show a larger relative variation.

The concentration-dependent effective-cluster interactions in the GPM, by contrast, do not suffer such an ambiguity[8,27] and the interactions can be computed, at least in principle, with arbitrary numerical precision.

C. Comparison of the magnitude of GPM and CWM interactions

Comparing cluster interactions from the CWM and effective-pair interactions from GPM is only possible to a limited extent because both types of interactions are defined in very different terms. To make this apparent, consider the ordering energy, defined by a variant of (1),

$$\Delta E^{\alpha}_{\mathrm{ord}} = E^{\alpha}_{\mathrm{tot}} - E^{\mathrm{dis}}_{\mathrm{tot}} \ . \tag{8}$$

TABLE IV. The CPA-disordered energy E_{dis}, and the first-, second-, third-, and fourth-nearest-neighbor effective-pair interactions (V_1^{GPM}, V_2^{GPM}, V_3^{GPM}, and V_4^{GPM}, respectively), in canonical units, for various alloys at equiatomic composition.

N_A-N_B	E_{dis}	V_1^{GPM}	V_2^{GPM}	V_3^{GPM}	V_4^{GPM}
{6-0}	−0.600 26	−0.009 394	−0.000 44	0.000 53	0.002 99
{7-1}	−0.571 33	0.042 661	−0.003 86	−0.002 21	−0.000 52
{8-2}	−0.421 81	0.081 560	−0.004 64	−0.002 50	−0.005 59
{9-3}	−0.144 42	0.043 652	0.000 86	0.000 20	−0.003 16
{10-4}	0.254 61	−0.019 133	0.005 18	0.002 80	0.004 47

From now on, for brevity, the superscript α, which indicates the configuration dependence, will be ignored. The ordering energy in the CWM is then, in a more explicit form, obtained by substitution of (3) and (5) into (8),

$$\Delta E_{\text{ord}}^{\text{CWM}} = \sum_{\gamma}^{\gamma_{\max}} V_{\gamma}^{\text{CWM}} [\xi_{\gamma} - (\xi_1)^{n_{\gamma}}] \ . \tag{9}$$

Comparing this expression with the GPM expression for the ordering energy [a variant of Eq. (6)],

$$\Delta E_{\text{ord}}^{\text{GPM}} = \sum_{s} q_s V_s^{\text{GPM}} \ , \tag{10}$$

makes clear that both types of interactions are used in quite different ways. In order to make a comparison possible, the CWM expression for the ordering energy will be matched to the corresponding GPM expression (as was suggested by Carlsson[29]). To this end both the q_s weight factors and the higher-order correlations (the latter by means of a superposition approximation) will be expressed in terms of pair and point correlations, and then the coefficients of these point and pair correlations in the GPM and CWM expressions for the ordering energy will be compared.

The q_s weight factors for the s nearest-neighbor shell, defined in (7), can be given exactly in terms of the coordination number z_s, the pair correlation $\xi_{s\text{-pair}}$, and the point correlation ξ_1,

$$q_s = \frac{z_s}{8}(\xi_{s\text{-pair}} - \xi_1^2) \ . \tag{11}$$

Truncating the summation in (10) at the second-neighbor shell and substituting (11) with $z_1 = 12$ and $z_2 = 6$ (fcc case) gives

$$\Delta E_{\text{ord}}^{\text{GPM}} = \tfrac{3}{2}(\xi_2 - \xi_1^2) V_1^{\text{GPM}} + \tfrac{3}{4}(\xi_3 - \xi_1^2) V_2^{\text{GPM}} \ . \tag{12}$$

The higher-order correlations in (9) can be approximated, by means of a superposition suggested by Carlsson,[29] as

$$\begin{aligned}\xi_{\gamma} = \langle \sigma_{p_1} \sigma_{p_2} \cdots \sigma_{p_n} \rangle &\approx \langle \sigma_{p_1} \sigma_{p_2} \rangle \langle \sigma \rangle^{n-2} + \langle \sigma_{p_1} \sigma_3 \rangle \langle \sigma \rangle^{n-2} + \cdots + \langle \sigma_{p_{n-1}} \sigma_{p_n} \rangle \langle \sigma \rangle^{n-2} - \left[\frac{n(n-1)}{2} - 1 \right] \langle \sigma \rangle^n \\ &= \xi_{p_1 p_2} \xi_1^{n-2} + \xi_{p_1 p_3} \xi_1^{n-2} + \cdots + \xi_{p_{n-1} p_n} \xi_1^{n-2} - \left[\frac{n(n-1)}{2} - 1 \right] \xi_1^n \ ,\end{aligned} \tag{13}$$

where n represents the number of lattice points in the γ cluster. Truncating (9) at the TO maximum cluster and using (13) for the higher-order correlations, the following (approximate) expression for the ordering energy is obtained:

$$\begin{aligned}\Delta E_{\text{ord}}^{\text{CWM}} \approx &(\xi_2 - \xi_1^2)(V_2^{\text{CWM}} + 3\xi_1 V_4^{\text{CWM}} + 2\xi_1 V_5^{\text{CWM}} + 6\xi_1^2 V_6^{\text{CWM}} + 5\xi_1^2 V_7^{\text{CWM}} + 4\xi_1^2 V_8^{\text{CWM}} + 8\xi_1^3 V_9^{\text{CWM}} + 12\xi_1^4 V_{10}^{\text{CWM}}) \\ &+ (\xi_3 - \xi_1^2)(V_3^{\text{CWM}} + \xi_1 V_5^{\text{CWM}} + \xi_1^2 V_7^{\text{CWM}} + 2\xi_1^2 V_8^{\text{CWM}} + 2\xi_1^3 V_9^{\text{CWM}} + 3\xi_1^4 V_{10}^{\text{CWM}}) \ .\end{aligned} \tag{14}$$

Matching (12) and (14) produces an approximate relationship between the GPM and CWM interactions,

$$\begin{aligned}V_1^{\text{GPM}} &\approx \tfrac{2}{3}(V_2^{\text{CWM}} + 3\xi_1 V_4^{\text{CWM}} + 2\xi_1 V_5^{\text{CWM}} + 6\xi_1^2 V_6^{\text{CWM}} + 5\xi_1^2 V_7^{\text{CWM}} + 4\xi_1^2 V_8^{\text{CWM}} + 8\xi_1^3 V_9^{\text{CWM}} + 12\xi_1^4 V_{10}^{\text{CWM}}) \ , \\ V_2^{\text{GPM}} &\approx \tfrac{4}{3}(V_3^{\text{CWM}} + \xi_1 V_5^{\text{CWM}} + \xi_1^2 V_7^{\text{CWM}} + 2\xi_1^2 V_8^{\text{CWM}} + 2\xi_1^3 V_9^{\text{CWM}} + 3\xi_1^4 V_{10}^{\text{CWM}}) \ .\end{aligned} \tag{15}$$

At the equiatomic composition, ξ_1 vanishes so that (15) can be simplified and rewritten as

$$\begin{aligned}V_2^{\text{CWM}} &\approx \tfrac{3}{2} V_1^{\text{GPM}} \\ V_3^{\text{CWM}} &\approx \tfrac{3}{4} V_2^{\text{GPM}} \ .\end{aligned} \tag{16}$$

Using (16) to compare the interactions in Tables III and IV ({9-3} alloy), a clear trend emerges: Both pair interactions are significantly larger in the CWM than in GPM. In case of the first- and second-nearest-neighbor-pair interactions the difference is of the order of 0.03 c.u. (0.14 eV) and 0.006 (0.027 eV), respectively. The differences between values of a typical CWM interaction obtained from various basis sets was much less, for the TO truncation only about 0.004 c.u. (0.018 eV). It is clear that the differences between GPM and CWM interactions are significant but at this point it is not possible to say which of the two methods produces the most accurate results.

D. Prediction of total energies with the GPM and the CWM

A description of phase equilibria in substitutional alloys from first principles is only possible if total energies of (ordered) phases can be predicted with sufficient accuracy. In order to predict the stable ordered structure at a given composition, for example, the error of the total energy must be significantly less than the energy difference between the competing phases.

As a measure of the energy difference between competing phases α and β, the following definition has been adopted: The energy difference squared $\Delta_{\alpha\beta}^2$ is the difference in the total energies of the phases α and β squared, averaged for 5 alloys, namely {6-0}, {7-1}, {8-2}, {9-3}, and {10-4}. In Table V the band energies for a series of competing phases are listed for this set of alloys. Energy differences for phase 3 and 4, 8 and 10, and 9 and 11, are respectively, 0.0074, 0.0073, and 0.0036 c.u. It is apparent that the band-energy differences of competing phases are of the order of 0.005 c.u. (0.02 eV). At this point, the question to be asked is, can the GPM and the

TABLE V. Band energies (in canonical units) of several competing phases obtained by recursion, for the set of alloys discussed in the text. For convenience the number associated with each ordered phase is given in the second row.

	$L1_0$	40	$L1_2$ (A_3B)	DO_{22} (A_3B)	$L1_2$ (AB_3)	DO_{22} (AB_3)
N_A-N_B	3	4	8	10	9	11
{6-0}	−0.590 725	−0.596 075	−0.867 459	−0.872 140	−0.281 020	−0.280 335
{7-1}	−0.592 724	−0.585 396	−0.802 562	−0.796 427	−0.350 596	−0.356 097
{8-2}	−0.465 551	−0.468 838	−0.622 609	−0.613 865	−0.212 544	−0.211 040
{9-3}	−0.165 181	−0.154 907	−0.306 676	−0.318 196	0.027 403	0.032 631
{10-4}	0.276 150	0.267 625	0.173 785	0.173 945	0.377 064	0.378 740

CWM predict total energies (i.e., band energies) with an error of the order of 0.005 c.u. (or less).

To address this question, both the GPM and the CWM were used to predict the band energy of the $L1_0$ phase in the 5 alloys already mentioned. The accuracy of the GPM or the CWM is defined in a similar fashion as the energy difference Δ, that is, as the root of the mean of the differences between predicted and exact (i.e., obtained directly with the recursion technique) band energies squared. Predictions with the GPM were made by substituting the data in Tables IV and VI into (1) and (10), and predictions with the CWM were based upon Table II and (3) and on band-energy data obtained by recursion.

The errors produced by both methods at various levels of approximation are shown in Table VII. The zeroth level of the GPM, that is, approximating the band energy by only the CPA disordered energy, gives an error that corresponds [per definition, see Eq. (8)] to an averaged value of the ordering energy. This averaged value of the ordering energy will be of use in Sec. E.

The first level of the GPM, in which the band energy is approximated by the sum of the contributions of the disordered energy (CPA) and the first-neighbor-pair interaction V_1, is almost an order of magnitude more accurate than the zeroth approximation. Moreover, at this level the accuracy is about the same as the energy difference of competing structures. The GPM with V_1 only is therefore already useful in the computation of phase equilibria.

Adding more (pair) interactions does not produce as drastic an improvement in the prediction of the band energy as was realized before. As a matter of fact the results with V_1 and V_2 have about the same error as the results with V_1-V_4. This is not surprising, since we observed in Sec. III A, that the pair interactions beyond the first neighbor do not converge rapidly in the GPM. An interesting observation is that the GPM in its most accurate form (V_1-V_4) consistently gives too low values for the band energy of the ordered phase. We will return to this observation in Sec. III E. In the majority of cases, the GPM is just about accurate enough to allow prediction of the ground-state properties, as was concluded elsewhere too.[28]

The CWM in the tetrahedron truncation yields generally less impressive results. Using a variety of basis sets (1,2,4,8,9, 1,2,6,8,9, and 1,2,5,6,7) generates errors which are generally several times greater than the energy differences of competing phases. It appears that the 1,2,4,8,9 basis set performs reasonably well, but that can be misleading because prediction of other ordered structures (such as 12 and 13) is much less accurate. When cluster interactions are computed from a basis set with more ordered structures than there are interactions (overdetermined basis set), the situation improves. Using an overdetermined basis set T:1,2,4–13, in which 5 interactions are computed from band energies of 12 structures, an accuracy is achieved comparable to (but still not as good as) what is obtained with the GPM. With T:1–13 as basis set, the $L1_0$ band energy is, strictly speaking, not

TABLE VI. Shell weight factors q_s, as defined by (7), for a number of ordered structures. N_r refers to the number associated with each ordered structure.

N_r	Structure	q_1	q_2	q_3	q_4
1 or 2	fcc	0	0	0	0
3	$L1_0$	$-\frac{1}{2}$	$\frac{3}{4}$	-1	$\frac{3}{2}$
4	40	$-\frac{1}{2}$	$\frac{1}{4}$	1	$-\frac{1}{2}$
5	$L1_1$	0	$-\frac{3}{4}$	0	$\frac{3}{2}$
6 or 7	$MoPt_2$	$-\frac{1}{3}$	0	$\frac{2}{3}$	$-\frac{1}{3}$
8 or 9	$L1_2$	$-\frac{3}{8}$	$\frac{9}{16}$	$-\frac{3}{4}$	$\frac{9}{8}$
10 or 11	DO_{22}	$-\frac{3}{8}$	$\frac{5}{16}$	$\frac{1}{4}$	$\frac{1}{8}$

TABLE VII. Errors in the total energies (in canonical units) for the $L1_0$ phase predicted with the GPM and CWM at various levels. "Level" refers to (1) in case of the GPM, the number of pair interactions considered, and (2) in case of the CWM, the T or TO truncation and the basis set used to compute the interactions.

Method	Level	Error (c.u.)
GPM	$E_{\text{dis}}^{\text{CPA}}$ only	0.0259
GPM	V_1 only	0.0059
GPM	V_1 and V_2	0.0045
GPM	V_1-V_4	0.0043
CWM	Ti:1,2,4,8,9	0.0074
CWM	T:1,2,6,8,9	0.0317
CWM	T:1,2,5,6,7	0.0201
CWM	T:1,2,4–13	0.0066
CWM	T:1–13	0.0036
CWM	TO:1,2,5–13	0.0137
CWM	TO:1,2,4–13	0.0130
CWM	TO:1–13	0.0000

TABLE VIII. Disordered energies (in canonical units) obtained with the CPA and with the CWM for a number of alloys at equiatomic composition.

$N_A - N_B$	CPA	T:1,2,3,8,9	T:1–13	TO:1–13
{6-0}	−0.600 26	−0.576 591	−0.581 777	−0.588 117
{7-1}	−0.571 33	−0.569 927	−0.566 477	−0.562 657
{8-2}	−0.421 81	−0.420 105	−0.417 882	−0.414 103
{9-3}	−0.144 42	−0.136 650	−0.136 496	−0.137 650
{10-4}	0.254 61	0.276 262	−0.272 820	0.269 771

predicted since this band energy value was used in the computation of the interactions. It is no surprise that in such a case high accuracies are found. Increasing the number of interactions is not very successful as is demonstrated by the disappointing accuracies obtained with the TO truncation. Basis set TO:1,2,5–13, which is not overdetermined, is more accurate than similar tetrahedron basis sets, but only by a factor of 2 or so. It appears that the degree of overdetermination of the basis set is very important since basis sets TO:1,2,5–13 and TO:1,2,4–13 have greater error than those obtained by using a T:1,2,4–13 basis set. The overdetermined TO:1–13 basis set does not really predict the $L1_0$ band energy, and due to a peculiarity of the correlation matrix the $L1_0$ band energies are reproduced exactly.

E. Comparison of the disordered energy from the CPA and from the CWM

In order to examine how the disordered energies from the CPA and from the CWM compare, computations with three basis sets have been performed: T:1,2,3,8,9, T:1–13 and TO:1–13. Table VIII shows that the CWM consistently gives less negative values for the disordered energy than the CPA does. This appears curious since CWM predictions of ordered configurations ($L1_0$ in Sec. III D) are just as often overestimated as underestimated. It must be that the CPA systematically yields too negative values for the disordered energy. This is in agreement with the finding (in Sec. III D) that the GPM in the most accurate procedure (using $V_1 - V_4$) consistently gave too negative values for the band energy. A very rough estimate of the accuracy of the CPA disordered energy can be found by comparing the two differences: (1) The difference between the CWM predicted band energy of an ordered phase with the actual value, and (2) the difference between the CWM predicted band energy of a disordered configuration with the CPA band energy. For the Ti:1,2,4–13 basis set, one finds that it predicts the band energy of the $L1_0$ structure with an average error of 0.0066 c.u., whereas the difference averaged of the predicted disordered energy and the CPA band energy is as large as 0.0124 c.u. (at equiatomic composition). Assuming that the CWM describes the disordered configuration with the same accuracy as it describes an ordered configuration, it follows that the extra error must be incurred by the inaccuracy in the CPA disordered energy. This suggests that at $c=0.5$ the error in the CPA disordered band energy can be of the order of 0.006 c.u.

F. Prediction of ordering energies and calculation of phase diagrams

An important feature of phase diagrams is the occurrence and range of stability of ordered phases. The temperature range of an ordered phase is determined by the order-disorder temperature, which in turn is more or less proportional to the ordering energy of the ordered phase. Accurate prediction of the ordering energy is therefore a requirement if a realistic first-principles calculation of a phase diagram is desired.

In Fig. 4 the ordering energy of the $L1_0$ phase is shown as a function of the number of d electrons of the B species ($N_B = N_A - 6$). The energies are computed by 3 methods; (1) by subtracting the CPA disordered energy from the total energy of the $L1_0$ phase (recursion CPA), (2) with the GPM using V_1 to V_4, and (3) with the CWM using a basis set T:1–13. The recursion CPA is probably the most accurate because the CPA is regarded as very precise (although not exact). The GPM and the CWM produce results that correspond well with the recursion CPA, although the GPM deviations at low N_B and the CWM digresses at high N_B. It is remarkable that the or-

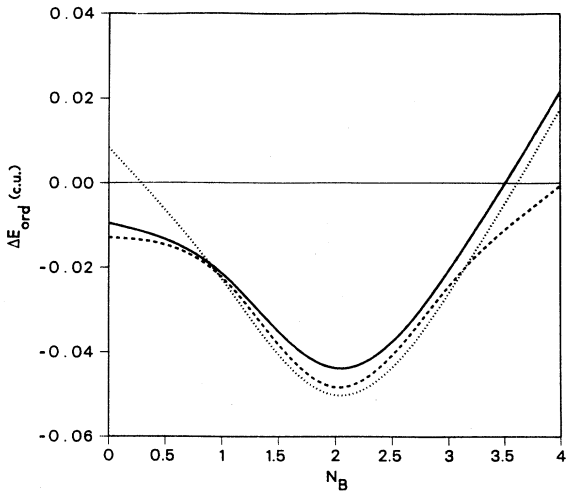

FIG. 4. The ordering energy ΔE_{ord} of the $L1_0$ phase in canonical units as a function of N_B ($N_B = N_A - 6$), computed with three different methods: (i) the solid line represents the recursion—CPA, (ii) the dotted line designates the GPM result, and (iii) the dashed line is computed with the tetrahedron CWM (T:1–13).

dering energies from the GPM and the CWM are actually closer to each other than either of them is to the recursion CPA.

In Sec. III D we saw that the ordering energy is typically of the order of 0.025 c.u. (0.1 eV), which can be verified by inspection of Fig. 4, so that a precision of about 0.0025 c.u. in the ordering energy is needed to predict an order-disorder temperature with an error of 10%. Neither the GPM nor the CWM appears to attain that accuracy at the levels of approximation considered in this study.

Assuming that the ordering energy has about the same error as the total energy (given in Table VII), it follows that the most accurate procedures, the GPM with the first-neighbor-pair interaction only (or with higher-neighbor-pair interactions) and the CWM with T:1–13 or TO:1–13 basis sets, are capable of predicting ordering energies (and hence order-disorder temperatures) with errors of about 20%. Many CWM procedures, however, which obtain interactions from smaller basis sets, will not be nearly as precise. In certain unfortunate cases the error in the ordering energy is expected to be of the same order as the ordering energy itself (see in Table VII T:1,2,5,6,7 and T:1,2,6,8,9).

To illustrate this point, the phase diagram of the {9-3} alloy in the tetrahedron approximation of the Cluster Variation Method has been computed with interactions obtained from four different procedures: By using (i) the GPM first-nearest-neighbor effective pair interaction V_1^{GPM} and by using the CWM with basis sets, (ii) T:1,2,3,8,9 and (iii) T:1,2,4,10,11, and (iv) T:1,2,3,9,10 (see Figs. 5(a)–5(d)]. The basis set T:1,2,3,9,10 corresponds to the most stable phases for the {9-3} alloy (see Table V). CWM interactions employed in this computation are listed in columns *a*, *b*, and *c* of Table III. Wide variations in order-disorder temperatures are displayed by the CWM phase diagrams. Table VII strongly suggests that the T-CWM with a basis set of 5 structures is

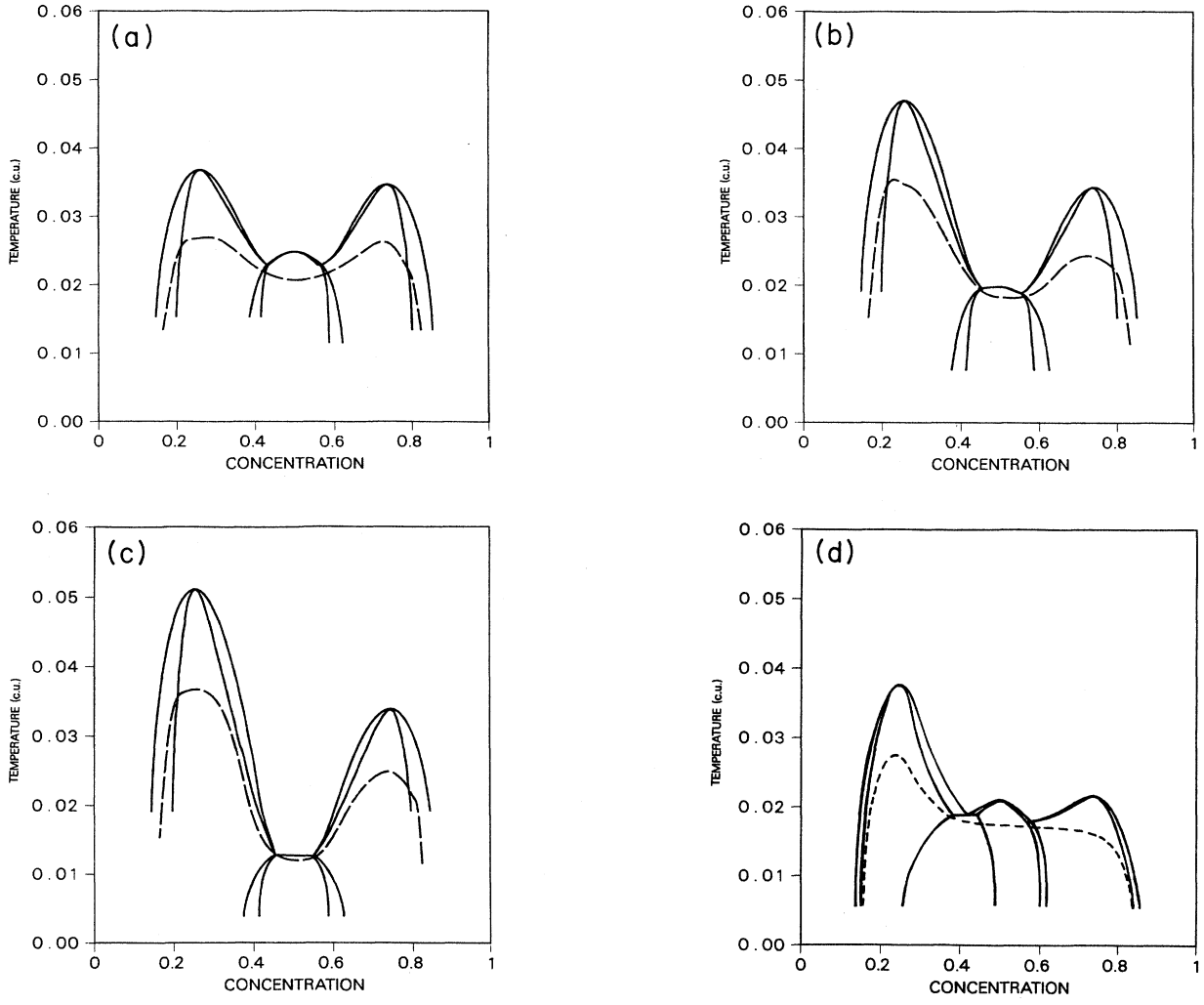

FIG. 5. Equilibrium fcc order-disorder phase diagrams for an alloy with $N_A=9$, $N_B=3$, and $\delta_d=0.8$, calculated in the tetrahedron approximation of the CVM. The cluster interactions used for diagrams (a), (b), and (c) are indicated in Table III, and the concentration-dependent effective-pair interaction used for (d) is computed with the GPM (the value at $c=0.5$ is listed in Table IV). the dashed curve indicates the [100] ordering spinodal. The temperature is expressed in canonical units (1 c.u. $\approx$ 52 000 K).

much less accurate than the GPM with nearest-neighbor effective-pair interactions only. We expect, therefore, that the phase diagram obtained with the GPM to be the most accurate among the four.

The conclusion is that phase diagrams can be computed with a reasonable accuracy with both methods, with the stipulation that the CWM can be relied upon only in case the basis set contains a rather large number of ordered structures (at least about ten in this study).

IV. CONCLUSION

The GPM was shown to be a useful method for the computation of phase diagrams and phase equilibria in general. The convergence of the GPM effective-pair interactions is generally very good up to the first-nearest-neighbor level only, but at that level many aspects of phase equilibrium are already accurately described. Going beyond the first-nearest-neighbor level is not a straightforward matter because the more distant pair interactions do not decay rapidly. The convergence breaks down, for both the GPM and the CWM, in alloys where the ordering energy is small. Within the GPM, at least a formal remedy exists, namely by retaining multisite terms in the perturbative expansion (2) for the ordering energy.[27,40]

The CWM was found to be a convenient and flexible method which could be extended easily to take into account volume (or more general, lattice parameter) dependence. Unfortunately, the CWM exhibited some troublesome features.

The terms of the "CWM equation" (3) do exhibit convergence, although at any particular truncation important cluster interactions can be overlooked. The CWM cluster interactions are basis set dependent and hence, interactions will vary within a certain range. For interactions which have large numerical values, such a variation produces only a small relative change, but for the numerically small interactions this variation can result in changes of sign. It was found that CWM interactions, after casting them in a "GPM" form, differ considerably from the GPM values. The difference between CWM and GPM interactions is much larger than the variation between the CWM interactions computed with different basis sets.

Regarding the accuracy of predicted total energies and ordering energies, the GPM was generally found to be superior to the CWM. If a sufficiently large set of ordered structures (about 10) is used for the computation of the CWM interactions, the accuracy of the CWM approaches that obtained with the GPM. It was shown that using the CWM with tetrahedron truncation with only five phases in the basis set is not very reliable for computing accuracy phase diagrams.

We conclude that phase diagrams can be computed with a reasonable accuracy with both methods, with the stipulation that the CWM can be relied upon only in case the basis set contains a rather large number of ordered structures (at least about ten in this study). Moreover, our computations suggest that the CPA has a tendency to result in disordered energies which are too negative.

We believe these conclusions to be model independent. Hence, we expect that similar conclusions will be obtained from a forthcoming study based on highly accurate *ab initio* KKR-CPA-GPM and full-potential linearized augmented-plane-wave (FLAPW) -CWM calculations. One should point out that although this study was restricted to binary substitutional transition metal alloys, similar conclusions can be drawn when the GPM and the CWM are applied within a tight-binding scheme to the problem of vacancy nitrogen, carbon ordering in transition-metal nitrides and carbides.[41]

ACKNOWLEDGMENT

This work was performed under the auspices of the U.S. Department of Energy by the Lawrence Livermore National Laboratory and by the Lawrence Berkeley Laboratory under Contract No. W-7405-ENG-48. One of the authors (M.S.) gratefully acknowledges Professor D. de Fontaine for encouragement and computer resources during the initial stages of this study.

APPENDIX: INTRODUCING VOLUME DEPENDENCE IN THE CWM

Total-energy computations for a particular ordered structure α with cubic symmetry have only one degree of freedom, the lattice parameter r or, completely equivalent, the molar volume v. Calculating $E^{\alpha}_{\rm tot}$ for various volumes v reveals that, in the vicinity of the equilibrium volume v^{α}_0, $E^{\alpha}_{\rm tot}$ has a volume dependence that is well described by a parabola of the form

$$E^{\alpha}_{\rm tot}(v)=E^{\alpha}_{\rm tot}(v^{\alpha}_0)+\frac{B^{\alpha}}{2}\frac{(v-v^{\alpha}_0)^2}{v^{\alpha}_0}\ , \tag{A1}$$

where $E_{\rm tot}(v_0)$ is the total energy at the equilibrium volume, and where B represents the bulk modulus. Hence, by fitting the total-energy values computed at various volumes to (A1), the equilibrium total energy, the equilibrium volume (or lattice parameter), and the bulk modulus are found. The volume dependence can be made more explicit by rewriting (A1) as

$$E^{\alpha}_{\rm tot}(v)=\varepsilon^{(0),\alpha}+\varepsilon^{(1),\alpha}v+\varepsilon^{(2),\alpha}v^2\ , \tag{A2}$$

where

$$\varepsilon^{(0),\alpha}=E^{\alpha}_{\rm tot}(v^{\alpha}_0)+\tfrac{1}{2}B^{\alpha}v^{\alpha}_0\ ,$$

$$\varepsilon^{(1),\alpha}=-B^{\alpha}\ ,$$

$$\varepsilon^{(2),\alpha}=\frac{B^{\alpha}}{2v^{\alpha}_0}\ .$$

When the configuration α is used as a vector index, (A2) can be expressed in matrix form as

$$\begin{bmatrix} E^{\alpha_1}_{\rm tot}(v) \\ E^{\alpha_2}_{\rm tot}(v) \\ E^{\alpha_3}_{\rm tot}(v) \\ \vdots \end{bmatrix} = \begin{bmatrix} \varepsilon^{(0),\alpha_1} & \varepsilon^{(1),\alpha_1} & \varepsilon^{(2),\alpha_1} \\ \varepsilon^{(0),\alpha_2} & \varepsilon^{(1),\alpha_2} & \varepsilon^{(2),\alpha_2} \\ \varepsilon^{(0),\alpha_3} & \varepsilon^{(1),\alpha_3} & \varepsilon^{(2),\alpha_3} \\ \vdots & \vdots & \vdots \end{bmatrix} \begin{bmatrix} 1 \\ v \\ v^2 \end{bmatrix}\ ,$$

or, in shorthand

$$\mathbf{E}^{\mathrm{tot}}(v)=\underline{\varepsilon}\cdot\mathbf{v} \ . \tag{A3}$$

Combining (A3) and (4) in matrix form then yields

$$\mathbf{V}(v)=\underline{\xi}^{-1}\mathbf{E}_{\mathrm{tot}}(v)=\underline{\xi}^{-1}\underline{\varepsilon}\cdot\mathbf{v}=\underline{\mu}\mathbf{v} \ ,$$

where

$$\underline{\mu}=\underline{\xi}^{-1}\underline{\varepsilon}=\begin{bmatrix} \mu_{\gamma_1}^{(0)} & \mu_{\gamma_1}^{(1)} & \mu_{\gamma_1}^{(2)} \\ \mu_{\gamma_2}^{(0)} & \mu_{\gamma_2}^{(1)} & \mu_{\gamma_2}^{(2)} \\ \mu_{\gamma_3}^{(0)} & \mu_{\gamma_3}^{(1)} & \mu_{\gamma_3}^{(2)} \\ \vdots & \vdots & \vdots \end{bmatrix} .$$

Hence, the volume dependence of the cluster interactions obeys a simple parabolic expression,

$$V_\gamma(v)=\mu_\gamma^{(0)}+\mu_\gamma^{(1)}v+\mu_\gamma^{(2)}v^2 \ . \tag{A4}$$

Volume-dependent interactions like those given by (A4) can be included easily into CVM free-energy functionals.[25,30] It is then possible to examine changes in the lattice parameter as a function of composition and state of order.

[1]R. Kikuchi, Phys. Rev. **81**, 988 (1951).
[2]J. M. Sanchez, F. Ducastelle, and D. Gratias, Physica **128A**, 334 (1984).
[3]K. Binder, J. L. Lebowitz, M. H. Phani, and M. H. Kalos, Acta Metall. **29**, 1655 (1981).
[4]K. Binder, in *Monte Carlo Methods in Statistical Physics,* Vol. 7 of *Topics in Current Physics,* edited by K. Binder (Springer, Berlin, 1986), p. 1.
[5]V. Heine and D. Weaire, Solid State Phys. **24**, 249 (1970).
[6]B. L. Gyorffy and G. M. Stocks, Phys. Rev. Lett. **50**, 374 (1983).
[7]A. Gonis, X. A. Zhang, A. J. Freeman, P. Turchi, G. M. Stocks, and D. M. Nicholson, Phys. Rev. B **36**, 4630 (1987), and references therein.
[8]F. Ducastelle and F. Gautier, J. Phys. F **6**, 2039 (1976).
[9]J. W. D. Connolly and A. R. Williams, Phys. Rev. B **27**, 5169 (1983).
[10]A. A. Mbaye, L. G. Ferreira, and A. Zunger, Phys. Rev. Lett. **58**, 49 (1987).
[11]L. G. Ferreira, A. A. Mbaye, and A. Zunger, Phys. Rev. B **35**, 6475 (1987).
[12]P. Soven, Phys. Rev. **156**, 809 (1967).
[13]B. Velicky, S. Kirkpatrick, and H. Ehrenreich, Phys. Rev. **175**, 747 (1968).
[14]F. Gautier, J. van der Rest, and F. Brouers, J. Phys. F **5**, 1884 (1975).
[15]F. Gautier, F. Ducastelle, and J. Giner, Philos. Mag. **31**, 1373 (1975).
[16]J. van der Rest, F. Gautier, and F. Brouers, J. Phys. F **5**, 2283 (1975).
[17]G. Treglia, F. Ducastelle, and F. Gautier, J. Phys. F **8**, 1437 (1978).
[18]A. Bieber, F. Gautier, G. Treglia, and F. Ducastelle, Solid State Commun. **39**, 149 (1981).
[19]P. Turchi, Thèse de Doctorat d'Etat, University of Paris VI, 1984 (unpublished).
[20]F. Ducastelle, in *Proceedings of the 1987 MRS Nato Advanced Study on Alloy Phase Stability,* edited by A. Gonis and G. M. Stocks (Kluwer Academic, Boston, 1989).
[21]T. Mohri, J. M. Sanchez, and D. de Fontaine, Acta Metall. **33**, 1171 (1985).
[22]J. Kanamori and Y. Kakehashi, J. Phys. (Paris) Colloq. **38**, C7-274 (1977).
[23]K. Terakura, T. Oguchi, T. Mohri, and K. Watanabe, Phys. Rev. B **35**, 2169 (1987).
[24]T. Mohri, K. Terakura, T. Oguchi, and K. Watanabe, Acta Metall. **36**, 547 (1988).
[25]M. Sluiter, D. de Fontaine, X. Q. Guo, R. Podloucky, and A. J. Freeman (unpublished).
[26]P. Turchi, M. Sluiter, and D. de Fontaine, Phys. Rev. B **36**, 3161 (1987).
[27]A. Bieber and F. Gautier, J. Phys. Soc. Jpn. **53**, 2061 (1984).
[28]A. Bieber and F. Gautier, Acta Metall. **34**, 2291 (1986), and references therein.
[29]A. E. Carlsson, Phys. Rev. B **35**, 4858 (1987).
[30]M. Sluiter, Ph.D. thesis, University of California Berkeley, 1988 (unpublished).
[31]S. Takizawa, K. Terakura, and T. Mohri, Phys. Rev. B **39**, 5792 (1989).
[32]M. Sluiter and P. Turchi, in *Proceedings of the 1987 MRS Nato Advanced Study Institute on Alloy Phase Stability,* edited by A. Gonis and G. M. Stocks (Kluwer Academic, Boston, 1989).
[33]A. Bieber and F. Gautier, Physica **107B**, 71 (1981).
[34]R. Haydock, Soild State Phys. **35**, 215 (1980).
[35]N. Beer and D. Pettifor, ψ_k Newsletter No. 4, 13 (Daresbury Lab., UK, 1982).
[36]P. Turchi, G. M. Stocks, W. H. Butler, D. M. Nicholson, and A. Gonis, Phys. Rev. B **37**, 5982 (1988).
[37]H. Shiba, Prog. Theor. Phys. **46**, 77 (1971).
[38]The {6-0} alloy is a hypothetical alloy since the *B* component has zero *d* electrons. Within the present context there is no reason to exclude this particular alloy.
[39]M. Sluiter, P. Turchi, and D. de Fontaine, J. Phys. F **17**, 2163 (1987).
[40]A. Bieber and F. Gautier, Acta Metall. **35**, 1839 (1987).
[41]J. P. Landesman, P. E. A. Turchi, F. Ducastelle, and G. Treglia, *Proceedings of the Materials Research Society Symposium,* edited by Th. Tsakalakos (North-Holland, Amsterdam, 1984), Vol. 21, p. 363; J. P. Landesman, G. Treglia, P. E. A. Turchi, and F. Ducastelle, J. Phys. (Paris) **46**, 1001 (1985).